Atomic Spectroscopy

Article

A New Micro-Solid Phase Extraction Using ZnMnAl LDH Nano-Sorbent for Cu and Ni Determination in Natural Water and Soil

Hassan Elzain Hassan Ahmed,[a,b,c,d] Zaki S. Seddigi,[e] and Mustafa Soylak[a,b,f,*]

[a] Faculty of Sciences, Department of Chemistry, Erciyes University, Kayseri, Türkiye

[b] Technology Research and Application Center (TAUM), Erciyes University, Kayseri, Türkiye

[c] Sudan Atomic Energy Commission (SAEC), Chemistry and Nuclear Physics Institute, Khartoum, Sudan

[d] Sudan University of Science and Technology (SUST), College of Science-Scientific Laboratories Department-Chemistry Section, Khartoum, Sudan

[e] Department of Environmental Health; Faculty of Public Health and Health informatics, Umm Al Qura University, Makkah, Saudi Arabia

[f] Turkish Academy of Sciences (TUBA), Ankara, Türkiye

Received: *January 03, 2024;* ***Revised:*** *February 20, 2024;* ***Accepted:*** *February 20, 2024;* ***Available online:*** *February 20, 2024.*

DOI: 10.46770/AS.2023.310

ABSTRACT: Layered double hydroxides (LDHs) are a class of materials that may be readily synthesized in a laboratory environment. This work successfully conducted the synthesis of a new nanomaterial (ZnMnAl LDH). The characterization of this material was accomplished utilizing many analytical techniques, including FTIR, XRD, SEM-mapping, and FE-SEM. ZnMnAl LDH was employed to separate and enrich Cu(II) and Ni(II) from soil and water samples. The Cu and Ni ions were eluted from ZnMnAl LDH nanoparticles by using 2 mL of 0.1 mol L^{-1} of HNO_3. The metal ions were quantified using flame atomic absorption spectrometry (FAAS). An investigation was conducted to examine the impact of many analytical factors on the efficiency of metal ions' extraction. These parameters include pH, sorbent amount, eluent volume, eluent concentration, sample volume, and possible interfering ions. The detection limits for Cu(II) and Ni(II) were found to be 0.74 and 0.52 µg kg^{-1}, respectively. In addition, the relative standard deviation (RSD%) for Cu(II) is 3.8 and for Ni(II) is 1.9. The linear range for both analytes is 50–1000 µg L^{-1}, and the preconcentration factor is 15 for both. The method's validation was verified by the analysis of certified reference materials, namely BCR-505 estuarine water and GBW07429 (GSS-15) soil. For soil samples, Ni(II) and Cu(II) concentrations vary from 9.8 to 62.8 mg kg^{-1} and 9.9 to 73.5 mg kg^{-1}, respectively. The technique described was used to quantify trace concentrations of copper (Cu) and nickel (Ni) in samples of both natural water and soil.

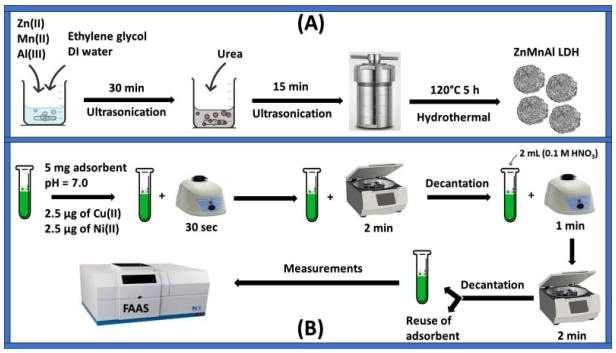

INTRODUCTION

Excessive copper and nickel concentrations in soil and drinking water endanger human health. Plants cultivated on metal-contaminated soil may absorb copper and nickel, resulting in greater levels in the crop. When people eat these contaminated crops, either directly or via products generated from animals fed on infected crops, they risk consuming high quantities of copper and nickel. Furthermore, groundwater may become polluted as a consequence of soil leaching, and drinking water from wells or groundwater reservoirs in locations with high metal concentrations may increase human exposure.[1-3] Copper may produce both acute and chronic symptoms, such as nausea and liver damage. Nickel exposure has been linked to cancer and respiratory difficulties. Plants may absorb these elements from the soil, impacting human exposure. Copper in drinking water may cause gastrointestinal problems, while nickel can harm the kidneys. Adherence to regulatory requirements and effective monitoring are critical for mitigating these health concerns.[3-6]

In order to identify and quantify trace amounts of metallic elements in a variety of environmental media, including water, air, sediments, soils, and living things, it is essential to analyze trace metals in environmental samples.[1,6-8] In the fields of agricultural and environmental sciences, trace metal detection in soil samples is crucial. By locating possible sources of pollution and calculating the degree of environmental damage, it is essential to the monitoring and assessment of the environment. In order to manage pollution caused by human activities such as mining and industrial operations, which may release hazardous trace metals into the environment, this knowledge is essential.[7,9-12] Trace metal analysis also involves understanding the condition of the soil. The presence of vital trace elements like zinc, copper, nickel, and iron directly impacts crop health and production; therefore, soil is a vital medium for plant development and agriculture. On the other hand, high concentrations of certain trace elements, such as iron or aluminum, may lower soil fertility. Accurate trace metal content analysis can help farmers and agronomists make decisions about how to manage the soil. For example, they can use soil amendments to make up for missing or too much of certain elements.[13-17]

Various techniques are employed in trace metal analysis based on the specific requirements of a study. Atomic absorption spectroscopy (AAS)[18-20] is a widely utilized method for quantifying individual trace metals by measuring light absorption at specific wavelengths. A lot of research and environmental assessments use inductively coupled plasma-mass spectrometry (ICP-MS),[21] ultraviolet-visible spectroscopy (UV-VIS),[22,23] and inductively coupled plasma-optical emission spectrometry (ICP-OES).[5,14] This is because they are very accurate and can find a lot of trace metals at once. X-ray fluorescence (XRF)[24] and neutron activation analysis (NAA)[21] are both non-destructive ways to quickly find out what elements are in soil samples in the field. Each method offers distinct advantages, enabling researchers to choose the most suitable approach based on the specific goals and characteristics of the study.

In order to significantly increase the sensitivity of trace metal measurements and quantify even ultra-trace concentrations, sample preparation procedures must be used prior to trace metal assessments in soil samples. [25-27] Furthermore, removing interfering compounds and reducing the influence of complex soil matrices yield more accurate and exact findings. Resource efficiency is also encouraged, as is adherence to environmental rules and the pursuit of particular research goals. Overall, these techniques are considered indispensable for obtaining the high-quality data required to assess the presence and impact of trace metals in soil, thereby informing environmental management, risk assessment, and regulatory compliance.[28-30] The micro-solid phase extraction (µ-SPE) approach provides various benefits over standard sample preparation methods. One prominent benefit is a considerable decrease in chemical and solvent use, which leads to better environmental and financial efficiency in studies. µ-SPE improves sensitivity, selectivity, and capacity to eliminate interfering matrix components, resulting in accurate and consistent findings. Furthermore, its small size and integration with analytical equipment make it versatile and suitable for sample preparation in both laboratory and field settings.[31-34]

One material that is appropriate for use in µ-SPE is layered double hydroxide (LDH) nanoparticles. They have many advantages, such as a large and adjustable surface area, excellent selectivity, and increased sensitivity.[35,36] Effective extraction and preconcentration of target analytes from complex sample matrices may be achieved by LDH-based µ-SPE, which also improves the sensitivity and accuracy of subsequent analytical tests by decreasing interference. In line with the principles of green chemistry, LDH-based µ-SPE has a speedy equilibrium, is compatible with different analytical methods, and reduces solvent usage. The analytical methods of researchers in many different domains may be improved with the help of LDH nanomaterials, which are adaptable tools. [35,37,38]

The selection of ZnMnAl LDH over alternative materials reflects a thoughtful consideration of multiple factors, emphasizing the novelty and advantages of our work. Adding Zn^{2+}, Mn^{2+}, and Al^{3+} to the LDH structure has a synergistic effect that makes it better at absorbing metal ions and gives Cu and Ni more strong sites to bind.[39,40] Zn, Mn, and Al are abundant and cost-effective elements, making ZnMnAl LDH a practical choice for large-scale environmental analysis. The cost-effectiveness of these elements enhances the feasibility and scalability of the proposed method.[40] In previous research and existing literature, ZnMnAl LDH was not synthesized and used in µ-SPE applications. This makes it a novel adsorbent for Cu(II) and Ni(II) extraction. This study has developed a new nanomaterial (ZnMnAl LDH), to selectively extract and preconcentrate trace levels of Cu(II) and Ni(II) from natural water and soil samples using µ-SPE followed by FAAS detection. The method was verified and applied to real samples analysis. ZnMnAl LDH nanomaterial offer several advantages for the separation and preconcentration of heavy metals, including enhanced adsorption efficiency, selective extraction capabilities, improved sensitivity, reduced interference, efficient and rapid processing, and positive environmental and health-related outcomes. Thes nanoparticles can effectively extract Cu(II) and Ni(II) from natural water and soil samples.

EXPERIMENTAL

Chemicals and instrumentals. All chemicals utilized in this study were of analytical reagent (AR) grade purity and were obtained from Merck (Darmstadt, Germany). The water employed in the study was double-distilled deionized water with a resistivity

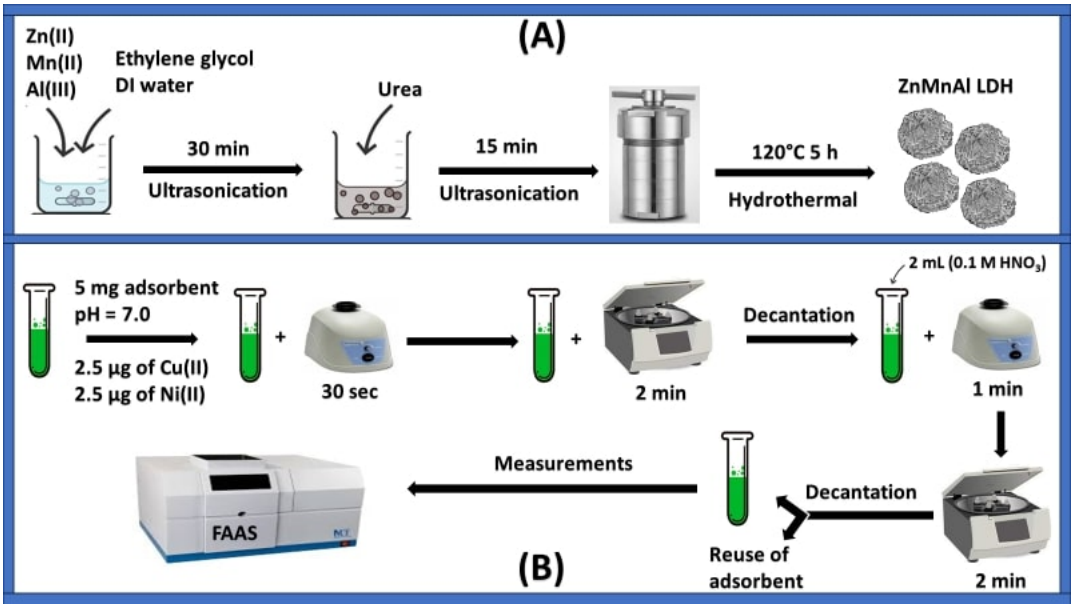

Fig. 1 Schematic representation of synthesis method of ZnMnAl LDH (A) and the µ-SPE method (B).

of 18.2 MΩ cm, obtained from Millipore. Stock solutions of Cu(II) and Ni(II) with a concentration of 1000 mg L^{-1} were procured from Labsert Lab. San. Tic. Ltd. Sti. (Mersin, Turkey). Matrix ion solutions were prepared at various concentrations. CRMs such as BCR-505 estuarine water and GBW07429 (GSS-15) soil CRMs were obtained from the Joint Research Centre (Geel, Belgium) and the National Research Center for Certified Reference Materials (NRCCRM) of China, respectively. The pH values were adjusted using phosphate, acetate, and ammonium buffer solutions. The following chemicals were bought from Merck in Darmstadt, Germany: aluminum nitrate nonahydrate, manganese nitrate hexahydrate, zinc nitrate hexahydrate, sulfuric acid (98%), nitric acid (65%), urea, ammonia solution (25%), ethylene glycol, sodium hydroxide, hydrochloric acid (37%), and ethyl alcohol. They were used to prepare the nanocomposite and the real samples's test. Buffer solutions containing phosphate, acetate, and ammonium were employed to optimize the pH of the solutions.

A flame atomic absorption spectrometer model contrAA 800 with a xenon arc lamp was used to measure the levels of Cu(II) and Ni(II). The solutions were shaken using a WhirliMixer Vortex Shaker Cyclone Mixer model 12665. Separation of the solid phase from the solutions was achieved using a Nuve NF400 (4×50 mL/4100 rpm) model centrifuge. Characterization of the materials was performed using the FT-IR model Perkin-Elmer Spectrum 400, the XRD model Bruker AXS D8, and the SEM model LEO 440 SEM.

Synthesis of ZnMnAl LDH. The hydrothermal method was used for the synthesis of the nanomaterial. 1.5 g of zinc nitrate hexahydrate, 1.45 g of manganese nitrate hexahydrate, and 1.88 g of aluminum nitrate nonahydrate were dissolved in a mixture of 35 mL of ethylene glycol and 15 mL of deionized water (DI). Ultrasonication was employed for 30 minutes to ensure complete dissolution of the above salts. Subsequently, 4.4 g of urea was added and sonicated for an additional 15 min. The resulting solution was then transferred to a 100-mL Teflon-lined stainless-steel autoclave and placed in an oven at 120°C for a duration of 5 hours. Following this, the autoclave was allowed to cool to room temperature, and the product was separated through centrifugation. The obtained nanomaterial was washed with DI three times and with ethanol two times. Finally, the resulting product was dried at 80°C for a period of 12 h.[41] Fig. 1A presents the graphical abstract of the synthesis procedure.

Extraction method. A 30 mL solution was prepared by combining 2 mL of phosphate buffer with a pH of 7.0, 2.5 µg of Cu(II), and 2.5 µg of Ni(II) in a centrifuge tube. To this mixture, 5 mg of ZnMnAl LDH nanoparticles were added, and the volume was completed with DI water. The contents of the tube were thoroughly mixed using a vortex for 30 s. The tubes were then placed in a centrifuge operating at 4100 rpm for 2 min to separate the resulting two phases using the decantation method (Fig. 1B). To release the adsorbed Cu(II) and Ni(II) from the sorbent, 2 mL of 0.1 M HNO_3 was added to the solid phase, vortexed for 1 min, and then centrifuged for 2 min. Finally, the eluted analytes were measured using FAAS.

Application to real samples. The proposed method was tested on natural water and soil samples. Natural water samples were

collected from Sivas, Yozgat, and Kocasinan (cities in Turkey) and preserved in glass bottles. 25.0 mL was taken from each sample, and the standard addition method was used with varying concentrations of Cu(II) and Ni(II). The method described in section of Extraction method was applied. The BCR-505 estuarine water was used directly after taking 10 mL, and then the described procedure was applied.

Ten samples of soil were taken from various sites in Mecca, Saudi Arabia, at a depth of 10 centimeters. Under controlled laboratory circumstances, the samples were transferred to dry glass containers and allowed to air-dry. The dried materials were first ground using a mortar, then passed through a 0.5-mm sieve. 1.0 g of each sample was taken and digested using a hot-plate digestion technique with Aqua Regia (a mixture of concentrated HCl and concentrated HNO_3 in a 3:1 volume ratio) at 100 °C for 1 h.[16] For the GBW07429 (GSS-15) soil CRMs, 500 mg was weighed and digested following the same procedure as the soil samples. The pH was adjusted to around 6, and the volumes were completed to 30 mL. The developed method was then applied to determine the Cu(II) and Ni(II) concentrations in soil samples using FAAS.

RESULTS AND DISCUSSION

Characterization of ZnMnAl LDH nanoparticles

In Fig. 2(i), the FT-IR spectra of ZnMnAl LDH nanoparticles display a prominent peak at 727 cm^{-1}, which indicates the stretching vibration of M-O (metal oxide) bonds. This unique peak is essential to the structural composition of the synthesized material, giving important information on the bonding interactions between metal cations (Zn, Mn, and Al) and oxygen atoms. The vibration mode at 727 cm^{-1} indicates strong metal-oxygen linkages (C-Zn-O, C-Mn-O, and C-Al-O) in the LDH structure, which contributes to the nanoparticles' stability and integrity. The absorption peaks at 3446, 1630, and 1403 cm^{-1} in the spectra of ZnAl LDH and MnAl LDH were found in earlier studies.[42,43] These are caused by the interlayer water molecules stretching, the brucite-like layer H_2O bending, and the nitrate stretching. The IR spectrum of ZnMnAl LDH also shows the same peaks. A broad peak at 3290 cm^{-1} was also observed, signifying a combination of the stretching vibrations arising from hydrogen bonding between water molecules and the metal hydroxyl groups within the hydroxide layers of the brucite sheets, as well as interlayer water molecules. Moreover, distinct peaks at 1634, 1049, and 1030 cm^{-1} were indicative of bending vibrations linked to the interlayer water molecules, involving C=O, C-O, and CO-O-CO interactions.[36,44] The peak observed at 2111 cm^{-1} corresponds to the stretching vibrations of the C≡N functional group.[41] The synthesized LDH exhibited characteristic peaks at 2934 and 2882 cm^{-1}, associated with C-H stretching groups, as well as a distinct peak at 1376 cm^{-1}, attributable to C-H bending groups.[44,45]

The XRD pattern of the ZnMnAl LDH is presented in Fig. 2(ii), revealing distinct diffraction peaks indicative of its crystalline structure. Specifically, the diffraction peaks observed at 2θ angles of 12.81°, 24.37°, 33.90°, 39.88°, 57.44°, 60.21°, and 63.11° correspond to the crystallographic planes (003), (009), (015), (018), (1010), (110), and (113), respectively, within the synthesized LDH structure. These peak positions and their intensities are consistent with the well-defined crystalline structure of ZnAl LDH.[44,46] Furthermore, Fig. 2(ii) also displays the prominent diffraction peaks characteristic of the MnAl LDH. These peaks occur at 2θ angles of 18.917°, 32.47°, 36.98°, 41.04°, 44.01°, and 53.81°, corresponding to the crystallographic planes (006), (012), (101), (104), (107), and (0111), respectively. These distinctive peaks further confirm the crystalline nature of the MnAl LDH structure.[45,47]

The synthesized ZnMnAl LDH underwent characterization through scanning electron microscopy (SEM) to investigate its crystalline structure and morphology. In Fig. 2(iii), as represented, micrographs of ZnMnAl LDH are displayed at various levels of magnification (a, b, c, and d). These images reveal that the samples possess a distinctive spherical shape-mode morphology with prominent bumps.[48] Each of these bumps can be attributed to either a single crystal or the assembly of a few crystalline grains. The growth of LDH grains predominantly occurs along two specific directions, giving rise to this unique shape. Importantly, a careful examination of the crystal surfaces demonstrates homogeneity, with no noticeable macroscopic defects.[49]

SEM-EDX analysis, as illustrated in Fig. 2(iv) (A-C), provides insights into the elemental composition of the prepared nanoparticles. This analysis confirms that the spherical shapes and the elemental components of the ZnMnAl LDH are consistent with those in the SEM images and ZnMnAl LDH, respectively.[48,50] Furthermore, the SEM-EDX study not only corroborates the information derived from the SEM images but also serves as evidence of the successful synthesis of these novel nanoparticles, reaffirming its distinct spherical shape-mode morphology with significant bumps.

The SEM-mapping image of ZnMnAl LDH in Fig. 2(v) provides evidence that the nano-sorbent was synthesized successfully. The elements, namely Zn, Mn, Al, C, and O, are distributed uniformly throughout the surface. The presence of carbon and oxygen suggests the existence of carbonate and hydroxide groups between the layers of the LDH, which could contribute to its adsorption properties. The quality and homogeneity of the ZnMnAl LDH nano-sorbent are further validated by the uniform distribution of elements, which confirms its suitability for applications including μ-SPE.

Fig. 2 (i): Infrared spectra of ZnMnAl LDH; (ii): X-ray diffraction patterns of ZnMnAl LDH; (iii): Scanning electron microscopy (SEM) images of ZnMnAl LDH; (iv): SEM-EDX analysis (A & B) and element contents of ZnMnAl LDH (C); (v): SEM-Mapping image of ZnMnAl LDH.

Optimization study

Effect of pH. The primary determinant of the quantitative recovery of the analytes is the level of acidity or alkalinity. The importance of pH in obtaining quantitative recoveries becomes more significant in the metal sorption process when a ligand is not employed.[51,52] The % recovery of Cu(II) and Ni(II) ions on ZnMnAl LDH nanoparticles was investigated in the pH range of

Fig. 3 (i): Impact of pH; (ii): Impact of sorbent amount; (iii): Impact of adsorption and desorption times; (iv): Impact of sample volume; (v): Impact of eluent concentration on Ni(II); (vi): Impact of eluent volume; (vii): Times of sorbent use; (viii): Calibration curves of Cu(II) and Ni(II), (N = 3).

4.0–9.0 (Fig. 3(i)). The findings indicated quantitative recoveries were obtained in the pH range of 7.0–8.0. In this pH range, these ions are in a stable and soluble form, which optimizes their adsorption by the sorbent material. LDHs bind metal ions by electrostatic interactions with hydroxyl groups on the surface, hydrogen bonds, and coordination with the metal ions. Isomorphic

substitution is another crucial mechanism, involving the exchange of metal ions within the LDH lattice with those in the solution. Factors like ion size, charge, and valency influence this process. LDHs can also induce the precipitation of metal hydroxides when the concentration of metal ions exceeds their solubility limit, resulting in metal hydroxides precipitating onto the LDH surface and facilitating the efficient removal of metal ions from the solution.[52-57] In this case only electrostatic interactions and isomorphic substitution may happen. Precipitation of metal hydroxides cannot happen due to this adsorption was done within neutral media (pH = 7.0). To fully comprehend the selectivity mechanism, more information on the synthesis and characterization of ZnMnAl LDH, binding affinities or selectivity coefficients, and competitive ion experiments during µ-SPE process optimization is needed. All subsequent experiments were conducted at a pH of 7.0, which was established as the optimal pH by using phosphate buffer solution.

Effect of sorbent amount. Different amounts of the new sorbent were examined to determine the optimal amount of sorbent for µ-SPE. The analyte concentration and sorbent capacity may both have an impact on the sorbent amount, which impacts extraction recovery. Optimization studies are required to achieve a balance between maximum extraction efficiency and the minimum sorbent amount.[52,53] The quantity of sorbent was optimized in the range of 5–25 mg to achieve substantial recovery values while minimizing sorbent usage. It was determined that the minimum amount of sorbent required for quantitative recovery of both analytes was 5 mg, as shown in Fig. 3(ii). This optimal quantity was subsequently used in further optimization studies.

Effect of adsorption and desorption times. The impact of reaction time is a vital factor in the adsorption and desorption processes, as shown in this research. This step emphasizes that, in general, the longer the analytes stay in contact with the solid phase, the higher the adsorption of analytes. Nevertheless, the connection between the variables is not linear, and there is a certain point at which increasing the adsorption period does not significantly enhance the recovery of the analyte. The solid phase has adsorbed all amounts of analytes where additional time cannot improve extraction, which is what causes this process. The discussion about the effect of reaction time focuses on the complex relationship between how well analytes are adsorbed and how long they interact with the solid phase.[58,59] The research examined adsorption and desorption periods ranging from 1.0 to 4.0 min. The approach consistently obtained quantitative recovery values for all investigated timeframes, showing its resilience over this time range. The key discovery was the identification of a 1-minute timeframe as the optimal period for both the adsorption and desorption processes of the examined metal ions. The meticulous evaluation of response time is crucial to maximizing the technique's effectiveness. A 1-minute duration creates a balanced state by ensuring sufficient interaction between the solid phase and analytes while preventing the occurrence of diminishing returns when all analyte ions are adsorbed. The optimal adsorption and desorption times are likely associated with the unique characteristics of the ZnMnAl LDH and its ability to rapidly adsorb and desorb trace metals.

Effect of sample volume. The sample volume used in µ-SPE is important because it affects the recovery and preconcentration factors. To determine the best sample volume, it is necessary to compare recovery values obtained from different volumes and select the one that gives the highest recovery and desired enrichment. This analysis helps identify the optimal sample volume for the rest of the analysis, ensuring the highest extraction efficiency in terms of recovery and enrichment.[56] The impact of sample volume on the recovery of metal ions from ZnMnAl LDH nanoparticles was investigated to achieve a high preconcentration factor for trace analyte ions. The study examined sample volumes ranging from 10 to 50 mL of sample solutions (Fig. 3(iv)). It was found that Ni(II) ions could be recovered quantitatively up to a sample volume of 50 mL, while Cu(II) ions could only be recovered up to 30 mL. Consequently, a sample volume of 30 mL was determined to be the optimal sample volume for both analyte metal ions and was employed for further experimentation.

Elution study. The concentration and volume of the eluent used in µ-SPE have a significant impact on the recovery values of the analytes of interest.[60] The choice of eluent is dependent on several factors, such as the properties of the analyte and sorbent, as well as the eluent's ability to efficiently desorb the target analytes from the solid phase while minimizing interference from other sample components. Solubility, selectivity, and compatibility with subsequent analysis methods should all be considered when selecting an eluent.[26,53] In this study, different concentrations and volumes of HNO_3 were studied, with the results depicted in Figs. 3(v) and 3(vi). Quantitative recovery values (>92%) for both analytes were observed for HNO_3 concentrations ranging from 0.1 to 3.0 mol L^{-1}. An eluent concentration of 0.1 mol L^{-1} was selected as the optimal concentration.

On the other hand, different volumes of eluent were also tested. The influence of eluent volume on recoveries was explored within the 1.0–5.0 mL range using 0.1 mol L^{-1} HNO_3 (Fig. 3(vi)). Quantitative recoveries were achieved for all analyte ions in the 2.0–5.0 mL range. Consequently, an eluent volume of 2.0 mL was selected as the optimal choice for subsequent experiments. The calculation of the preconcentration factor (PF) was performed as PF = initial sample volume (30.0 mL) / eluent volume (2.0 mL), resulting in a PF of 15.

Study of sorbent reusability. Reusability of the sorbent material in µ-SPE means that the sorbent may be regenerated and used again and again to extract the analytes of interest. Improving the extraction method's cost-effectiveness and sustainability relies on this aspect. The development of stable sorbent materials that retain

Table 1 Tolerance limits of interfering ions in determination of 2.5 µg of both Cu(II) and Ni(II) (N = 3)

Interferent	Added as	Ratio of interferent/analyte	Recovery, %	
			Cu(II)	Ni(II)
K^+	KCl	36,000	96 ± 5[a]	103 ± 2
Na^+	$NaNO_3$	60,000	102 ± 2	100 ± 5
Mg^{2+}	$Mg(NO_3)_2$	12,000	90 ± 2	98 ± 0
Ca^{2+}	$Ca(NO_3)_2$	10,000	97 ± 7	94 ± 4
Fe^{3+}	$Fe(NO_3)_3.9H_2O$	60	98 ± 2	98 ± 4
Al^{3+}	$Al(NO_3)_3.9H_2O$	60	102 ± 1	92 ± 5
Ag^+	$AgNO_3$	60	99 ± 4	96 ± 4
Cr^{3+}	$Cr(NO_3)_3$	60	100 ± 4	96 ± 1
Co^{2+}	$Co(NO_3)_2$	36	97 ± 3	100 ± 0
Pb^{2+}	$Pb(NO_3)_2$	36	99 ± 5	98 ± 0
Zn^{2+}	$Zn(NO_3)_2.6H_2O$	36	91 ± 6	93 ± 4
Cl^-	KCl	32,000	96 ± 5	103 ± 2
NO_3^-	$NaNO_3$	160,000	102 ± 2	100 ± 5
CO_3^{2-}	Na_2CO_3	6,000	97 ± 4	101 ± 1
SO_4^{2-}	Na_2SO_4	6,000	105 ± 3	101 ± 5
HPO_4^{2-}	$Na_2HPO_4.2H_2O$	14,000	97 ± 2	99 ± 4

[a] Mean ± Standard deviation.

their adsorption capabilities after several use cycles is a common area of research attention.[61,62] The reusability of ZnMnAl LDH without any treatment is illustrated in Fig. 3(vii). Until the third cycle, the adsorption efficiency remained constant at 102%–94% for both analytes. As shown in Fig. 3(vii), the adsorption efficiency for Ni(II) decreased after the third cycle (4th cycle, 85%) and peaked at 68% in the sixth cycle. This suggested that the adsorption sites present in ZnMnAl LDH were ineffective in facilitating the quantitative adsorption of Ni(II). Cu(II) exhibited an adsorption efficiency surpassing 90% until the fifth cycle of application. The adsorption efficiency subsequently decreased by less than 90%. This finding suggests that the ZnMnAl LDH exhibited a reusability of threefold for Ni(II) adsorption and fivefold for Cu(II) adsorption, both under ideal conditions.

Interference study. Studying the impact of common interfering ions on the extraction efficiency of the recovery values of the target analytes plays an important role in evaluating the suitability of the analytical method. The tolerance limit for an interfering ion was determined as the highest concentration at which no significant change in the analytical signal was caused (not exceeding ±5%).[38,63]The study of the effect of various interfering ions on the extraction and determination of the target analytes (Cu(II) and Ni(II)) was carried out. Solutions containing 2.5 µg of Cu(II) and 2.5 µg of Ni(II) were subjected to testing with different interfering ions. Table 1. displays the cations and anions that have not significantly affected by the extraction and determination processes. As a result, the selectivity of the proposed method for the extraction, preconcentration, and quantification of Cu(II) and Ni(II) is affirmed.

Analytical performance

A set of experiments was conducted under optimal conditions to determine the linear range (LR), limit of detection (LOD), limit of quantification (LOQ), relative standard deviation (%RSD), and enrichment factor (EF) using two calibration curves, one with the proposed method and one without. The R^2 values for Cu(II) and Ni(II) with the proposed method were found to be 0.9979 and 0.9958, respectively. The formula [3 * *SD*/m] was used to calculate the LODs for this method, where m is the calibration curve's slope and *SD* is the standard deviation of ten blank solutions. The LODs were determined to be 0.74 µg kg^{-1} for Cu(II) and 0.52 µg kg^{-1} for Ni(II). The LOQs were calculated as 3.33 times the LOD and were found to be 2.25 µg kg^{-1} for Cu(II) and 1.72 µg kg^{-1} for Ni(II). The preconcentration factors were 15 for Cu(II) and 25 for Ni(II), while the EFs were 14 and 28 for Cu(II) and Ni(II), respectively. The %RSDs within the LR of 50–1000 µg L^{-1} for both analytes (n = 3) were 3.8% for Cu(II) and 1.9% for Ni(II). The standard curves with linear equations were shown in Fig. 3(viii). The eluent volume and eluent concentration used for elution were 2 mL and 0.1 mole L^{-1}, respectively.

Application to real samples

The method was applied to natural water and soil samples for preconcentrating and measuring Cu(II) and Ni(II). The results are presented in Table 2 for water samples and in Table 3 for soil samples from Mecca. Table 2 shows the quantitative recovery values for both analytes from water samples. The recovery is between 92% and 106%, underscoring its reliability for Cu(II) and Ni(II) analysis in these water samples. Table 3 lists the measured concentrations of Cu(II) and Ni(II) in 10 different soil samples. The concentrations of Cu(II) range from 9.9 to 73.5 mg kg^{-1}, with an average concentration of approximately 29.3 mg kg^{-1}. The concentrations of Ni(II) range from 9.8 to 62.8 mg kg^{-1}, with an average concentration of approximately 35.3 mg kg^{-1}. Soil 1 and Soil 4 exhibited the highest concentrations of Cu(II) and Ni(II) respectively. Conversely, Soil 5 and Soil 6 had the lowest

Table 2. Cu(II) and Ni(II) levels in natural water samples (N = 3)

Water samples	Added, mg L^{-1}	Found, mg L^{-1}		Recovery, %	
		Cu(II)	Ni(II)	Cu(II)	Ni(II)
Sivas tap water	0	ND	ND	---	---
	0.200	0.201 ± 0.007 [a]	0.188 ± 0.011	101 ± 4	94 ± 6
	0.400	0.377 ± 0.007	0.350 ± 0.010	94 ± 2	88 ± 3
Yozgat tap water	0	ND	ND	---	---
	0.200	0.189 ± 0.005	0.179 ± 0.008	95 ± 2	90 ± 5
	0.400	0.369 ± 0.016	0.400 ± 0.012	92 ± 4	100 ± 3
Kocasinan tap water	0	ND	ND	---	---
	0.200	0.212 ± 0.010	0.191 ± 0.004	106 ± 5	96 ± 2
	0.400	0.393 ± 0.020	0.381 ± 0.010	98 ± 5	95 ± 3

[a] Mean ± Standard deviation; ND: No detection.

Table 3. Cu(II) and Ni(II) levels in soil samples, and statistical tests (N = 3)

Soil samples		Measured concentration, mg kg^{-1}		%RSD	
		Cu	Ni	Cu	Ni
Soil 1		73.5 ± 3.0[a]	35.4 ± 1.7	4.1	4.8
Soil 2		12.0 ± 0.2	31.7 ± 1.8	1.8	5.7
Soil 3		17.4 ± 0.8	46.7 ± 1.3	4.7	2.8
Soil 4		19.8 ± 0.7	62.8 ± 0.8	3.5	1.2
Soil 5		9.9 ± 0.8	31.1 ± 1.8	7.8	5.8
Soil 6		17.6 ± 0.5	9.8 ± 0.9	2.8	9.3
Soil 7		13.6 ± 0.3	28.8 ± 0.6	2.2	2.1
Soil 8		17.1 ± 0.4	44.4 ± 1.7	2.4	3.8
Soil 9		50.3 ± 0.6	31.9 ± 0.3	1.2	0.8
Soil 10		65.9 ± 1.8	33.1 ± 1.2	2.8	3.5
Statistical tests	**Correlation coefficient (r)**			-0.191	
	T-test	*p* value = 0.08		T-table value = 1.83	Confidence level = 95%

[a] Mean ± Standard deviation.

Table 4. Levels of Cu and Ni in CRMs after application of presented method (N = 3)

CRMs	Certified		Measured		Recovery, %	
	Cu	Ni	Cu	Ni	Cu	Ni
BCR-505 estuarine water, nmol kg^{-1}	29.4 ± 1.5[a]	24.1 ± 2.0	26.8 ± 1.9	22.9 ± 1.6	91	95
GBW07429 (GSS-15) soil, µg g^{-1}	37.0 ± 2.0	41.0 ± 1.0	36.3 ± 2.3	38.5 ± 2.0	98	94
T-test	*p* value = 0.45		T-table value = 1.9		Confidence level = 95%	

[a] Mean ± Standard deviation.

concentrations of Cu(II) and Ni(II) respectively, indicating potential lower levels of natural or human-induced metal contamination. Further analysis and comparison to regulatory guidelines are necessary to determine the significance of these concentrations in relation to environmental and human health impacts. A correlation coefficient (r) test was performed between Cu and Ni concentrations in soil samples. A value of -0.191 was obtained, which indicates a negative correlation between the concentration of analytes in soil samples. This negative correlation means that as copper levels tend to increase, nickel levels tend to decrease, and vice versa. However, the value of -0.191 suggests that this negative correlation is relatively weak.

A t-test was also utilized to find out if there is any statistical correlation between Cu and Ni levels in soil samples. In Table 3, with a p-value of 0.07959 and a significance level of 0.05, the null hypothesis is not rejected, indicating that there is no statistically significant correlation between Cu and Ni concentrations in soil samples.

The presented method was validated by using it on CRMs like BCR-505 estuarine water and GBW07429 (GSS-15) soil, as shown in Table 4. The test of CRMs for Cu and Ni in soil and estuarine water samples has produced results that validate the dependability and precision of the proposed method employed. The recovery values are quantitative and close to the certified values for both metals in both analytes. These results highlight the accuracy of the developed procedure. A T-test was also carried out on the certified and measured values. The t-test results, including the t-statistic and p-values, indicate that there is no statistically significant difference between the means of certified values and measured values. The data suggests that the means of the two groups are not significantly different at the chosen significance level of 0.05.

The µ-SPE technique has several advantages over other µ-SPE methods, as shown in Table 5. Most notably, it has lower LODs for Cu(II) and Ni(II) ions, making it more sensitive and able to detect even lower concentrations of these ions in samples.

Table 5. Comparison studies with different µ-SPE techniques for Cu(II) and Ni(II)

Technique	Sorbent used	Sorbent amount (mg)	LOD (µg L^{-1} or µg kg^{-1})	%RSD	PF/EF	Analysis technique	Ref.
SPE	TMA-co-DVB-co-AMPS	150	2.2 for Cu; 1.5 for Ni	<2.0	75	FAAS	[64]
SPE	MWCNTs	200	2.3 for Cu; 6.0 for Ni	<5.0	50	FAAS	[32]
SPE	MWCNTs-EDDA	15	0.14 for Cu; 0.21 for Ni	1.89-3.16	130	FAAS	[65]
µ-SPE	MMNP@HL	7	0.04 for Cu; 0.03 for Ni	2.1 & 2.2	11	FAAS	[66]
SPE	Silica gel-thiocyanatopropyl	120	1.9 for Cu	2.8	73	FAAS	[67]
SPE	XAD4-SAB	500	0.50 for Cu; 0.90 for Ni	<4.0	240	FAAS	[68]
µ-SPE	ZnMnAl LDH	5	0.74 for Cu; 0.52 for Ni	<4.0	15	FAAS	This work

Note: PTMA-co-DVB-co-AMPS: poly [prothymosin-alpha -co-divinylbenzene-co-2-acrylamido-2-methylpropane sulfonic acid]; MWCNTs: Multiwalled carbon nanotubes; EDDA: ethylenediamine N,N-diacetic acid; MMNP@HL: MCM-41 mesoporous-coated magnetite nano-particles@N-(4-methoxysalicylidene)-4,5-dinitro-1,2-phenylenediamine; SAB: salicylaldehyde benzoylhydrazone.

Additionally, the lower RSDs show that the method is more precise, which makes it more reproducible. Furthermore, it achieves relatively high PFs, making it particularly well-suited for analyzing samples with low concentrations of these ions. Using ZnMnAl LDH in µ-SPE is a good way to concentrate and study Cu(II) and Ni(II) ions in water and soil samples. It also has some unique benefits that make it the best µ-SPE method.

CONCLUSION

This research involved the successful synthesis and characterization of a new nanomaterial known as ZnMnAl LDH. For characterization, various analytical techniques, including FTIR, XRD, and FE-SEM, were employed. Additionally, the novel sorbent enabled the selective micro-solid phase extraction (µ-SPE) of Cu and Ni from natural water and soil samples. Validation was studied by applying the developed method to the CRMs, specifically BCR-505 estuarine water and GBW07429 (GSS-15) soil. Analyzing Cu and Ni in soil and estuarine water samples using these CRMs produced results that confirm the method's precision and reliability. The novel ZnMnAl LDH nano-sorbent for µ-SPE, combined with spectrometric detection, provides a sensitive, reliable, easy-to-use, cost-effective, and eco-friendly approach that is appropriate for the preconcentration and separation of Cu(II) and Ni(II) in routine analytical procedures.

AUTHOR INFORMATION

Prof. Mustafa Soylak is working on Environmental Analytical Chemistry, Nanotechnology, Nanomaterials, Nanocomposites, Separation/ Preconcentration Techniques including Solid Phase Extraction, Coprecipitation, Cloud point extraction, membrane filtration, speciation and microextraction of trace organic and inorganic species. Dr. Soylak has an h-index of 113 (Web of science). He has over 750 papers in Web of Science, 8 book chapters and reviews, two textbooks (in Turkish), one textbook on microextraction techniques (Elsevier, 2020). He is Editor-in-Chief of Comprehensive Sampling and Sample Preparation (Elsevier, 2023). He was visiting professor at King Saud University- Saudi Arabia on 2010-2016 and at Near East University-Cyprus on 2018-2019. He is now Professor at Erciyes University, Department of Chemistry, Kayseri-Turkey. He is the editorial board member of *Atomic Spectroscopy*, *Journal of Hazardous Materials*, *International Journal of Environmental Analytical Chemistry*, *Arabian Journal of Chemistry*, *Turkish Journal of Chemistry*, and *Journal of Nanostructure in Chemistry*. He has TUBITAK (Turkish Scientific and Technological Research Council) Encouragement Award in 2001. He is the recipient of the highest prestigious science award in Turkey, TUBITAK Science Award in 2020. He has also İlim Yayma Award from İlim Yayma Foundation in 2021. He has been a principal member of the Turkish Academy of Sciences (TUBA) since 2020. He has obtained a TÜBİTAK 2247-A National Fellowship for Outstanding Researchers (2021).

Corresponding Author

* M. Soylak

Email address: soylak@erciyes.edu.tr

Notes

The authors declare no competing financial interest.

ACKNOWLEDGMENTS

The authors are grateful for the financial support of the Unit of the Scientific Research Projects of Erciyes University (FYG-2023-13184).

REFERENCES

1. S. Saracoglu, K. O. Saygi, O. D. Uluozlu, M. Tuzen, and M. Soylak, *Food Chem*, 2007, **105**, 280–285. https://doi.org/10.1016/j.foodchem.2006.11.022
2. M. D. Mastromatteo, *J. Occup. Environ. Med.*, 1967, **9**, 127–136. https://www.jstor.org/stable/45004198
3. T. Zeinali, F. Salmani, and K. Naseri, *Biol. Trace Elem. Res.*, 2019, **191**, 338–347. https:// doi.org/10.1007/s12011-019-1637-6

4. R. Magaye, J. Zhao, L. Bowman, and M. I. N. Ding, *Exp. Ther. Med.*, 2012, **4**, 551–561. https://doi.org/10.3892/etm.2012.656
5. J. Wu, S. Lan, J. Sun, H. She, G. Wang, X. Wen, S. Zhou, B. Ying, X. Wang, and H. Wang *Food Anal. Methods*, 2023, **16**, 1655–1672. https://doi.org/10.1007/s12161-023-02528-y
6. V. Antunović, D. Blagojević, R. Baošić, D. Relić, and A. Lolić, *Environ. Monit. Assess.*, 2023, **195**, 596. https://doi.org/10.1007/s10661-023-11232-7
7. M. Hossain, D. Karmakar, S. N. Begum, S. Y. Ali, and P. K. Patra, *Microchem. J.*, 2021, **165**, 106086. https://doi.org/10.1016/j.microc.2021.106086
8. H. H. Özaytekin and M. Dedeoğlu, *Bull. Environ. Contam. Toxicol.*, 2023, **111**, 61. https://doi.org/10.1007/s00128-023-03818-1
9. F. U. Haque, F. Faridullah, M. Irshad, A. Bacha, Z. Ullah, M. Fawad, F. Hafeez, A. Iqbal, R. Nazir, A. F. Alrefaei, and M. H. Almutairi, *Land (Basel)*, 2023, **12**, 1894. https://doi.org/10.3390/land12101894
10. B. J. Alloway, Heavy Metals in Soils, 2012. Springer Science & Business Media. https://link.springer.com/book/10.1007/978-94-007-4470-7
11. M. Soylak and O. Turkoglu, *J. Trace Microprobe Tech.*, 1999, 17, 209–217. https://webofscience.clarivate.cn/wos/woscc/full-record/WOS:000080056100007
12. N. A. Kasa, N. K. Zeytinci, B. N. Aydin, and S. Bakirdere, *Chem. Pap.*, 2023, in press. https://doi.org/10.1007/s11696-023-03228-x
13. M. J. McLaughlin, B. A. Zarcinas, D. P. Stevens, and N. Cook, *Commun Soil Sci. Plant. Anal.*, 2000, **31**, 1661–1700. https://doi.org/10.1080/00103620009370531
14. A. Sungur, Y. Kavdir, H. Özcan, R. İlay, and M. Soylak, *Catena*, 2021, **197**, 104995. https://doi.org/10.1016/j.catena.2020.104995
15. A. Sungur, M. Soylak, and H. Özcan, *Environ. Earth Sci.*, 2016, **75**, 334. https://doi.org/10.1007/s12665-016-5268-3
16. A. Sungur, E. Temel, T. Everest, M. Soylak, and H. Özcan, *Arch. Agron. Soil Sci.*, 2023, **69**, 2677–2691. https://doi.org/10.1080/03650340.2023.2171019
17. T. D. Dinh, Q. L. Nguyen, M. D. Vu, T. M. H. Tran, T. H. N. Tran, M. H. Nguyen and T. D. Pham, *Colloid Polym. Sci.*, 2023, **301**, 1197–1207. https://doi.org/10.1007/s00396-023-05140-y
18. A. J. Yusuf, A. Galadima, Z. N. Garba, and I. Nasir, *Res. J. Chem. Sci.*, 2015, 5, 8-10. https://acfm.fafu.edu.cn/__local/7/09/92/DB82F9CD324D21154D5DE5BD164_AEC674AF_14C8B.pdf?e=.pdf
19. K. Parvizzad, M. A. Farajzadeh, and S. M. Sorouraddin, *Anal. Sci.*, 2023, **39**, 1493–1499. https://doi.org/10.1007/s44211-023-00365-x
20. Z. Erbas, R. Maulana, E. Yilmaz, S. Ozdemir, E. Kilinc, and M. Soylak, *Int. J. Environ. Anal. Chem.*, 2020, **100**, 992–1003. https://doi.org/10.1080/03067319.2019.1646737
21. S. Gaudino, C. Galas, M. Belli, S. Barbizzi, P. de Zorzi, R. Jaćimović, Z. Jeran, A. Pati, and U. Sansone, *Accreditation Qual. Assur.*, 2007, **12**, 84–93. https://doi.org/10.1007/s00769-006-0238-1
22. L. Yuan, X. Chen, L. Yao, and T. Pan, *Soil. Sediment Contam.*, 2024, 33, 115–138. https://doi.org/10.1080/15320383.2023.2185452
23. M. Soylak, U. Şahin, and L. Elçi, *Anal. Chim. Acta*, 1996, **322**, 111–115. https://doi.org/10.1016/0003-2670(95)00603-6
24. J. Q. McComb, C. Rogers, F. X. Han, and P. B. Tchounwou, *Water Air Soil Pollut.*, 2014, **225**, 2169. https://doi.org/10.1007/s11270-014-2169-5
25. M. Soylak, L. Elci, and M. Dogan, *J. Trace Microprobe Tech.*, 1999, 17, 149−156.
26. M. B. Arain, H. E. H. Ahmed, and M. Soylak, *Microchem. J.*, 2023, **195**, 109495. https://doi.org/10.1016/j.microc.2023.109495
27. D. Kara, A. Fisher, and S. J. Hill, *J. Hazard. Mater.*, 2009, **165**, 1165–1169. https://doi.org/10.1016/j.jhazmat.2008.10.111
28. M. Soylak, H. E. H. Ahmed, and A. N. Coban, *J. Food Compost. Anal.*, 2024, **125**, 105716. https://doi.org/10.1016/j.jfca.2023.105716
29. S. Bodur, S. Erarpat, Ö. F. Tutar, and S. Bakırdere, *J. Food Compost. Anal.*, 2023, **117**, 105144. https://doi.org/10.1016/j.jfca.2023.105144
30. C. F. Poole, Solid-phase extraction. Elsevier, 2019. https://doi.org/10.1016/C2018-0-00617-9
31. B. Buszewski and M. Szultka, *Crit. Rev. Anal. Chem.*, 2012, **42**, 198–213. https://doi.org/10.1080/07373937.2011.645413
32. E. Yilmaz and M. Soylak, *Environ. Monit. Assess.*, 2014, **186**, 5461–5468. https://doi.org/10.1007/s10661-014-3795-5
33. H. E. H. Ahmed, O. Ozalp, and M. Soylak, *J. Food Compost. Anal.*, 2023, **118**, 105163. https://doi.org/10.1016/j.jfca.2023.105163
34. H. E. H. Ahmed, Z. P. Gumus, and M. Soylak, *Anal. Lett.*, 2024, 57, 681–693. https://doi.org/10.1080/00032719.2023.2221754
35. V. dos S. A. Leite, V. R. L. Constantino, C. M. S. Izumi, J. Tronto, and F. G. Pinto, *New J. Chem.*, 2020, **44**, 10087–10094. https://doi.org/10.1039/C9NJ05771D
36. G. Starukh, O. Rozovik, and O. Oranska, *Nanoscale Res. Lett.*, 2016, **11**, 228. https://doi.org/10.1186/s11671-016-1402-0
37. Y.-L. Liu, J.-B. Zhou, R.-S. Zhao, and X.-F. Chen, *Anal. Bioanal. Chem.*, 2012, **404**, 1603–1610. https://doi.org/10.1007/s00216-012-6219-9
38. M. Rajabi, M. Abolhosseini, A. Hosseini-Bandegharaei, M. Hemmati, and N. Ghassab, *Microchem. J.*, 2020, **159**,105450. https://doi.org/10.1016/j.microc.2020.105450
39. X. Wang, Y. Lin, Y. Su, B. Zhang, C. Li, H. Wang, L. Wang, *Electrochim. Acta*, 2017, **225**, 263–271. https://doi.org/10.1016/j.electacta.2016.12.160
40. K. Li, S. Li, Q. Li, H. Liu, W. Yao, Q. Wang, and L. Chai, *J. Hazard. Mater.*, 2022, **427**, 127865. https://doi.org/10.1016/j.jhazmat.2021.127865
41. G. Nyongombe, G. L. Kabongo, I. T. Bello, L. L. Noto, and M. S. Dhlamini, *Energy Rep.*, 2022, 8, 1151–1158. https://doi.org/10.1016/j.egyr.2021.12.042
42. Y. Du, L. Liu, Y. Feng, B. Yang, and X. Wu, *RSC Adv.*, 2019, **9**, 39699–39708. https://doi.org/10.1039/C9RA08391J
43. F. Huang, S. Tian, Y. Qi, E. Li, L. Zhou, and Y. Qiu, *Materials*, 2020, **13**, 1951. https://doi.org/10.3390/ma13081951
44. P. Yazdani, E. Mansouri, S. Eyvazi, V. Yousefi, H. Kahroba, M. S. Hejazia, A. Mesbahi, V. Tarhriz and M. M. Abolghasemi, *Artif. Cells Nanomed B.*, 2019, **47**, 436–442. https://doi.org/10.1080/21691401.2018.1559182
45. Y. Du, L. Liu, Y. Feng, B. Yang, and X. Wu, *RSC Adv.*, 2019, **9**, 39699–39708. https://doi.org/10.1039/C9RA08391J
46. A. Li, H. Deng, C. Ye, and Y. Jiang, *ACS Omega*, 2020, **5**, 15152–15161. https://doi.org/10.1021/acsomega.0c01092

47. G. Mishra, B. Dash, S. Pandey, and P. P. Mohanty, *J. Environ. Chem. Eng.*, 2013, **1**, 1124–1130. https://doi.org/10.1016/j.jece.2013.08.031
48. G.-Y. Kang, Y. Chen, and J.-J. Li, *J. Inorg. Mater.*, 2016, **31**, 1230–1236. https://doi.org/10.15541/jim20160099
49. M. Richetta, L. Digiamberardino, A. Mattoccia, P. G. Medaglia, R. Montanari, R. Pizzoferrato, D. Scarpellini, A. Varone, S. Kaciulis, A. Mezzi, P. Soltani, and A. Orsini, *Surf. Interface Anal.*, 2016, **48**, 514–518. https://doi.org/10.1002/sia.5973
50. M. Shao, W. Hong, T. Zhu, X. Jiang, Y. Sun, and S. Hou, *RSC Adv.*, 2022, **12**, 26834–26845. https://doi.org/10.1039/D2RA04308D
51. A. A. Lashari, T. G. Kazi, J. A. Baig, H. I. Afridi, A. Lashari, and F. Kandhro, *Geoderma*, 2023, **437**, 116601. https://doi.org/10.1016/j.geoderma.2023.116601
52. H. E. H. Ahmed, A. M. A. Mohammed, and M. Soylak, *Food Chem.*, 2023, **428**, 136794. https://doi.org/10.1016/j.foodchem.2023.136794
53. H. E. H. Ahmed and M. Soylak, *J. Food Compost. Anal.*, 2023, **121**, 105396. https://doi.org/10.1016/j.jfca.2023.105396
54. M. Mabrouk, A. H. Moustafa, A. A. Gouda, H. E. Mohamed, A. M. Alshehri, M. M. Garoub, A. H. Al-Bagawi, and M. A. El-Attar, *Talanta Open*, 2023, **8**, 100275. https://doi.org/10.1016/j.talo.2023.100275
55. Q. Huang, Y. Chen, H. Yu, L. Yan, J. Zhang, B. Wang, B. Du and L. Xing, *Chem. Eng. J.*, 2018, **341**, 1–9. https://doi.org/10.1016/j.cej.2018.01.156
56. A. A. Gouda and S. M. Al Ghannam, *Food Chem*, 2016, **202**, 409–416. https://doi.org/10.1016/j.foodchem.2016.02.006
57. C. Duran, A. Gundogdu, V. N. Bulut, M. Soylak, L. Elci, H. B. Sentürk, and M. Tüfekci, *J. Hazard. Mater.*, 2007, **146**, 347–355. https://doi.org/10.1016/j.jhazmat.2006.12.029
58. L. B. Guimarães, L. S. G. Teixeira, F. A. C. Amorim, and F. de S. Dias, *Appl. Spectrosc. Rev.*, 2023, **58**, 545–561. https://doi.org/10.1080/05704928.2022.2066687
59. M. Soylak, A. H. Kori, and H. E. H. Ahmed, *Atom. Spectrosc*, 2023, **44**, 326-335. https://doi.org/10.46770/AS.2023.264
60. Y. E. Unsal, M. Tuzen, and M. Soylak, *J. AOAC Int.*, 2016, **99**, 534–538. https://doi.org/10.5740/jaoacint.11-0490
61. D. A. Gkika, A. C. Mitropoulos, and G. Z. Kyzas, *Sci. Total Environ.*, 2022, **822**, 153612. https://doi.org/10.1016/j.scitotenv.2022.153612
62. P. Suresh Kumar, W. W. Ejerssa, C. C. Wegener, L. Korving, A. I. Dugulan, H. Temmink, M. C. M. van Loosdrecht and G.-J. Witkamp, *Water Res.*, 2018, **145**, 365–374. https://doi.org/10.1016/j.watres.2018.08.040
63. H. Abdolmohammad-Zadeh, Z. Rezvani, G. H. Sadeghi, and E. Zorufi, *Anal. Chim. Acta*, 2011, **685**, 212–219. https://doi.org/10.1016/j.aca.2010.11.035
64. T. Daşbaşi, H. Muğlu, C. Soykan, and A. Ülgen, *J. Macromol. Sci. A*, 2018, 55, 288–295. https://doi.org/10.1080/10601325.2018.1424556.
65. M. A. Karimi, S. Z. Mohammadi, A. Hatefi-Mehrjardi, A. Mohadesi, and J. Yarahmadi, *J. Anal. Sci. Technol.*, 2015, 6, 25. https://doi.org/10.1186/s40543-015-0065-2
66. P. Azizi, M. Golshekan, S. Shariati, and J. Rahchamani, *Environ. Monit. Assess.*, 2015, 187, 185. https://doi.org/10.1007/s10661-015-4419-4
67. N. Manousi, A. Kabir, K. G. Furton, G. A. Zachariadis, and A. Anthemidis, *Separations*, 2021, 8, 100. https://doi.org/10.3390/separations8070100
68. G. Alpdoğan, *Toxicol. Environ. Chem.*, 2016, 98, 179–188. https://doi.org/10.1080/02772248.2015.1115508